

PDF hosted at the Radboud Repository of the Radboud University Nijmegen

The following full text is a publisher's version.

For additional information about this publication click this link.

<http://hdl.handle.net/2066/84033>

Please be advised that this information was generated on 2020-09-18 and may be subject to change.

Size dependent magnetic moments and electric polarizabilities of free Tb, Ho, and Tm clusters

J. Bowlan,^{1,a)} C. N. van Dijk,² A. Kirilyuk,² A. Liang,¹ S. Yin,¹ Th. Rasing,² and W. A. de Heer¹

¹*School of Physics, Georgia Institute of Technology, Atlanta, Georgia 30332, USA*

²*Institute for Molecules and Materials, Radboud University Nijmegen, 6525 ED Nijmegen, The Netherlands*

(Presented 19 January 2010; received 31 October 2009; accepted 27 January 2010; published online 27 April 2010)

Stern–Gerlach deflection measurements have been performed on rare earth clusters Tb_N , Ho_N , and Tm_N ($N \leq 40$) at cryogenic temperatures ($T \leq 77$ K). Tb_N and Ho_N share a common size dependence in their magnetic moments. They both exhibit common “magic number” sizes which show reduced net magnetic moments, similar to previous observations for Gd and Dy clusters. Tm_N have smaller magnetic moments that do not differ significantly between cluster sizes. The reduced net magnetic moments are evidence that the atomic moments are canceled by a canted or antiferromagnetic alignment. Electric deflection experiments reveal that Tm_N have electric dipole moments and show an enhanced response to an electric field compared to Tb_N and Ho_N . © 2010 American Institute of Physics. [doi:10.1063/1.3350904]

I. INTRODUCTION

Molecular beam measurements, using the Stern–Gerlach (SG) deflection technique, have provided valuable insights into the properties of small magnetic clusters. This technique allows the magnetic response of a cluster to be measured as a function of the number of atoms (N), magnetic field, and temperature in the absence of any support. The technique is now well developed and has been applied to a variety of cluster systems. It was used to reveal the evolution of ferromagnetism from the atom to the bulk in three-dimensional transition metal clusters¹ and in various magnetic alloy cluster systems. The SG technique not only provides accurate magnetic moments, but also insight into the magnetic anisotropy.²

The rare earth metals with partially filled $4f$ shells have large atomic moments and show a variety of interesting magnetic phases at low temperature, due to the oscillatory nature of the indirect exchange interaction.³ These magnetic properties are highly sensitive to the lattice geometry, so it is interesting to investigate rare earth clusters where the majority of atoms are on the surface.

II. EXPERIMENTAL METHODS

A. Apparatus

The SG deflection technique used to measure the magnetic moments of Tb_N , Ho_N , and Tm_N is briefly described next (see Fig. 1).¹ The clusters are produced in a cryogenic laser vaporization source.⁴ A pulsed laser produces a minute cloud of metal vapor in a small, cryogenically cooled chamber (20–300 K) filled with helium where the clusters are formed and fully thermalize (for further details, see Ref. 5). The clusters then pass through a small opening in the chamber to form a cluster beam. In the collision-free beam, the

total energy and angular momentum of each individual cluster is fixed. The energy (and angular momentum) distributions of the ensemble of clusters in the beam reflect the temperature of the source, as revealed in the measured ensemble properties (i.e., average deflections and deflection distributions). Note that at the lowest temperatures used in our experiments (15–50 K), the majority of the clusters are in their electronic and vibrational ground states.^{6,7}

The cluster beam is deflected in the inhomogeneous magnetic field of the SG magnet (magnetic field $B=0-1$ T and transverse field gradient $dB/dz=0-345$ T/m). Subsequently, the cluster beam is irradiated with a pulse of ionizing light from an excimer laser, which singly ionizes a small fraction of the clusters in the beam. The cluster beam is detected using a position sensitive time of flight mass spectrometer, which simultaneously measures both the mass and the deflection of all of cluster sizes produced.

B. Magnetic deflection

The cluster deflections δ are proportional to the net magnetization M_N , and depend on the cluster mass m , velocity v , and a calibration constant for the deflection magnet K ,

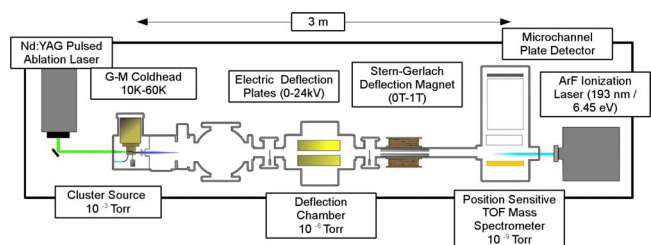


FIG. 1. (Color online) Schematic diagram of the cluster beam experiment. Clusters are produced in the pulsed laser vaporization source (to the left) at a repetition rate of 20 Hz. Clusters are deflected in an inhomogeneous electric or magnetic field and the deflected clusters are measured in the position sensitive time of flight mass spectrometer (right).

^{a)}Electronic mail: jbowlan@gmail.com.

$$\delta = K \frac{\bar{M}_N \frac{dB}{dz}}{mv^2}. \quad (1)$$

\bar{M}_N for a free cluster in a magnetic field is defined to be the average projection of the magnetic moment in the direction of the applied magnetic field. The magnetization depends on the coupling of the cluster's intrinsic magnetic moment μ_N to the cluster body. The physical cause of such a coupling is the spin-orbit interaction, just as for magnetocrystalline anisotropy in a bulk material. Specifically, if the coupling is weak and the spin is relatively unhindered (for $\mu_N B \ll kT$), then the cluster beam will deflect uniformly with little broadening. In this case, the Langevin susceptibility relates μ_N and \bar{M}_N . In the low field limit, this relation has the form

$$\bar{M}_N \approx \frac{\mu_N^2 B}{3kT}. \quad (2)$$

Note that the spin relaxation mechanisms that give rise to superparamagnetism in the bulk do not apply to metal clusters at low temperature ($T \ll T_{\text{Debye}}$), due to the lack of a suitable heat bath for relaxation. Nevertheless, as shown in detail by Ref. 6, the ensemble average deflection still follows a Langevin-like behavior. If the intrinsic moment is strongly coupled to the cluster axis, then the magnetization will depend on the rigid body motion of the cluster in the deflection field. In this case, \bar{M}_N will still follow a Langevin-like form, but with a smaller slope in the low field limit and a slower saturation.² It is also noteworthy that this strong coupling regime (also called a locked-moment regime) predicts that a significant fraction of the clusters will be deflected toward the low field direction which we do not observe (as in Ref. 8). Therefore, to facilitate a comparison between cluster sizes and across elements, we report the moments derived from the Langevin susceptibility at low temperatures.

C. Electric deflection

The electric deflection measurements are in all respects similar to the magnetic deflection measurements, only the inhomogeneous magnetic field is replaced by an inhomogeneous electric field ($E \approx 6 \times 10^7$ V/m). The electric deflections are caused by two factors: the electronic polarizability α of the cluster and a permanent electric dipole moment p . α gives rise to an induced dipole moment $P = \alpha E$. For simple metal clusters $\alpha \approx 4\pi\epsilon_0 R^3$, where R is the cluster radius (see Ref. 9). This causes a uniform deflection of the cluster beam. The permanent dipole moment p (if present) also gives a contribution to the deflection, as well as a broadening of the beam. Consequently, the electric deflections are given by the formula⁹

$$d = \left(\alpha + \kappa \frac{p^2}{kT_R} \right) \frac{E \nabla E}{mv^2} K_e, \quad (3)$$

where T_R is the rotational temperature, κ is a constant which depends on the cluster's axes of inertia, and K_e is a calibration constant for the deflection field.

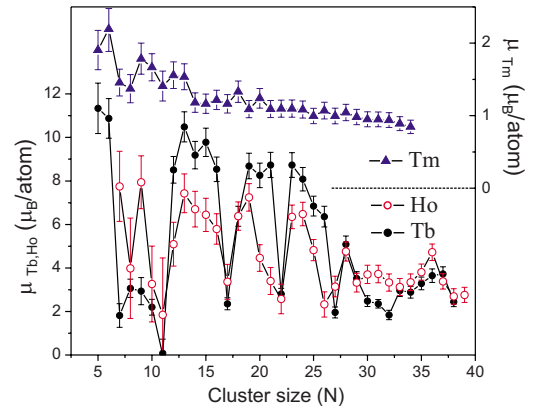


FIG. 2. (Color online) Total magnetic moments for Tb, Ho, and Tm clusters μ_N divided by the number of atoms, derived from the Langevin susceptibility [Eq. (2)]. Both Tb_N and Ho_N show a similar oscillatory trend in their moments as a function of size, which suggests that they have a common geometric structure. Tm_N behaves differently, with significantly reduced moments and no oscillatory trend with cluster size. The beam temperature is 77 K for Tb_N , 54 K for Ho_N , and 20 K for Tm_N . Note that this is only the *net* magnetic moment for the cluster and reduced values do not necessarily imply reduction in the atomic moments.

III. RESULTS

A. Magnetic magic numbers

The values of μ_N extracted from the Langevin susceptibility for Tb_N , Ho_N , and Tm_N are shown in Fig. 2. It is apparent from the plot that certain cluster sizes for both Tb and Ho show vastly reduced moments. These “magic number” minima are seen at $N=11, 17, 22, 27$, and possibly 32. Since our experiment is only sensitive to the net magnetic moment of the entire cluster, we cannot determine whether reduced net moment is due to the reduction in the atomic $4f$ moments or a cancellation of the atomic moments by a canted or antiferromagnetic alignment. Earlier theoretical work on Gd clusters has emphasized the importance of canted spin arrangements.¹⁰ Tm_N does not follow the same trend as Tb and Ho clusters. All Tm_N clusters show reduced values of μ_N compared to both the atomic and bulk ($7.14 \mu_B$) values,³ implying all Tm_N clusters have a canted or antiferromagnetic arrangement of atomic moments.¹¹

B. Electric response

The polarizabilities of Tb_N and Ho_N (Fig. 3) are consistent with a classical conducting sphere model, while Tm_N is anomalous and shows large enhancements. Under identical conditions, Tm_N shows much larger deflections compared to Tb_N and Ho_N . This enhancement is large ($20\text{--}40 \text{ \AA}^3/N$) and is reduced at higher temperatures (not shown). This enhancement is due to an unscreened electric dipole moment. Similar effects have been observed, for example, in Pb clusters.¹²

IV. CONCLUSION

Common size dependence in the magnetic properties of Tb and Ho clusters have been observed. These trends show minima at specific magic number cluster sizes which have been observed in previous measurements on Gd, Tb, and Dy clusters (only $N=22$ was observed for Gd).^{8,13–16} The com-

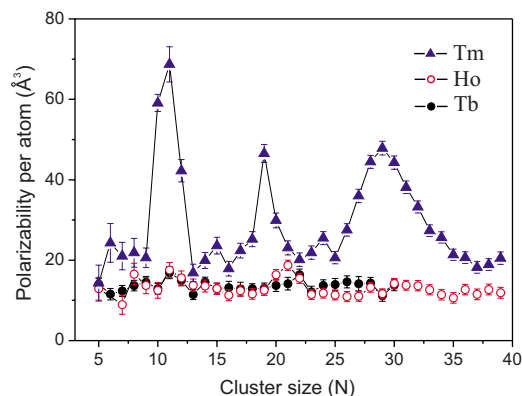


FIG. 3. (Color online) Electric polarizabilities α_N of rare earth clusters (Tb_N , Ho_N , and Tm_N). Tb and Ho have polarizabilities consistent with metallic sphere behavior. The polarizability of Tm is anomalously enhanced in several size ranges. This enhancement reflects the contribution to the deflection of a permanent dipole moment.

mon trend across these four elements (Gd, Dy, Tb, and Ho) suggests that these clusters have a common geometric structure like the bulk materials. The reduced moments of the magic number clusters can be most simply explained by a canted or antiferromagnetic arrangement of the $4f$ moments.

Tm_N , however, does not follow the same size dependence in μ_N as the other materials investigated. All Tm_N clusters show significantly reduced moments, implying that all sizes have an antiferromagnetic or canted spin structure. The electric dipole moments imply that the $6s$ electrons must be partially localized because the polarization is unscreened. The screening response is closely related to the Ruderman-Kittel-Kasuya-Yosida (RKKY)³ interaction, so this observation has implications for the nature of the indirect exchange interaction.

While these measurements do not directly reveal the nature of the magnetic order or exchange in the rare earth clusters, they strongly constrain the possibilities and hopefully will prove helpful for theoretical studies.

ACKNOWLEDGMENTS

Funding for this research was provided by the U.S. NSF Grant No. 4106B21, the Dutch Nanotechnology initiative NanoNed and EC FP7 contributions under Grant Nos. NMP3-SL-2008-214469 (UltraMagnetron) and N 214810 (FANTOMAS).

- ¹I. Billas, A. Chatelain, and W. de Heer, *Science* **265**, 1682 (1994).
- ²G. Bertsch and K. Yabana, *Phys. Rev. A* **49**, 1930 (1994).
- ³J. Jensen and A. Mackintosh, *Rare Earth Magnetism* (Oxford University Press, New York, 1991).
- ⁴X. Xu, S. Yin, R. Moro, and W. de Heer, *Phys. Rev. Lett.* **95**, 237209 (2005).
- ⁵P. Milani, *Rev. Sci. Instrum.* **61**, 1835 (1990).
- ⁶X. Xu, S. Yin, R. Moro, and W. de Heer, *Phys. Rev. B* **78**, 054430 (2008).
- ⁷S. Pokrant, *Phys. Rev. A* **62**, 051201(R) (2000).
- ⁸D. Gerion, A. Hirt, and A. Châtelain, *Phys. Rev. Lett.* **83**, 532 (1999).
- ⁹W. de Heer and V. Kresin, e-print arXiv:0901.4810 (2009).
- ¹⁰D. Pappas, A. Popov, A. Anisimov, B. Reddy, and S. Khanna, *Phys. Rev. Lett.* **76**, 4332 (1996).
- ¹¹V. Cerovski, S. Mahanti, and S. Khanna, *Eur. Phys. J. D* **10**, 119 (2000).
- ¹²S. Schäfer, S. Heiles, J. Becker, and R. Schafer, *J. Chem. Phys.* **129**, 044304 (2008).
- ¹³D. Douglass, A. Cox, J. Bucher, and L. Bloomfield, *Phys. Rev. B* **47**, 12874 (1993).
- ¹⁴D. Douglass, J. Bucher, and L. Bloomfield, *Phys. Rev. Lett.* **68**, 1774 (1992).
- ¹⁵J. Bucher and L. Bloomfield, *Int. J. Mod. Phys. B* **7**, 1079 (1993).
- ¹⁶A. Cox, D. Douglass, J. Louderbeck, A. Spencer, and L. Bloomfield, *Z. Phys. D: At., Mol. Clusters* **26**, 319 (1993).